

THE KARLSRUHE  $4\pi$  BaF<sub>2</sub> DETECTOR

K. Wisshak, K. Guber, F. Käppeler, J. Krisch, H. Müller, G. Rupp, F. Voss

Kernforschungszentrum Karlsruhe, Institut für Kernphysik,  
D-7500 Karlsruhe, Federal Republic of Germany

**Abstract:** The  $4\pi$  array of 42 BaF<sub>2</sub> crystals which has been set up at Karlsruhe over the past three years is intended for precise measurements of neutron capture cross sections in the energy range  $3 < E_n < 200$  keV, primarily for astrophysical applications. We present the essential features of the detector, e.g. mechanical construction, setup of the individual detector modules, and the stabilisation of the entire system, which is operated as a calorimeter summing all gamma-rays of the capture cascade. Time and energy resolution of the individual detector modules are 0.4 ns and 5.7% at 2.5 MeV gamma-ray energy, while the corresponding values for the system as a whole are 0.5 ns and 7.1%, respectively. The performance of the detector under experimental conditions is demonstrated in various test measurements on gold samples.

(BaF<sub>2</sub> scintillators,  $4\pi$  gamma-ray detection, neutron capture cross sections,  
 $3 < E_n < 200$  keV)

1. Introduction

The Karlsruhe  $4\pi$  BaF<sub>2</sub> detector<sup>1,2</sup> has been completed by the end of 1987. It will be used for precise measurements of neutron capture cross sections in the energy range from 3 to 200 keV, primarily for astrophysical applications. Such data are essential for our understanding of stellar nucleosynthesis of the heavy elements in the so-called s-process<sup>3</sup> (s = slow neutron capture).

The Karlsruhe detector is the second setup which operates as a calorimeter for identifying neutron capture events via the complete summation of the capture cascade. The first approach was the  $4\pi$  detector ROMASCHKA<sup>4</sup>, consisting of 48 blocks of NaI(Tl) of 180 l total volume, thus allowing in principle for high efficiency at good intrinsic resolution in gamma-ray energy. However, the large amount of <sup>10</sup>B, which is used to shield the crystals from sample scattered neutrons and the thick cannings of the crystals severely degraded the energy resolution. Therefore, only multiplicity spectra are recorded with this detector.

Replacing NaI(Tl) by BaF<sub>2</sub> scintillator crystals makes the Karlsruhe detector about 10 to 100 times less sensitive to scattered neutrons. This means that no <sup>10</sup>B shield is required in this case. Moreover, the chemical stability of BaF<sub>2</sub> does not require any canning of the individual crystals except a 0.3 mm thick reflector, consisting of two layers of PTFE foil (poly-tetra-fluor-ethylene), aluminum foil, and black tape. In conjunction with the well defined neutron spectra that are obtained from nuclear reactions, it will be possible with the new setup to measure not only the multiplicity but also the sum energy of the capture gamma-ray cascades, and hence to derive the capture cross sections with high precision. The fact that all individual detector modules see the sample under identical solid angles as well as the excellent time resolution are additional virtues of the Karlsruhe detector. In the following, the main features of the setup are presented together with first results from test measurements on gold samples.

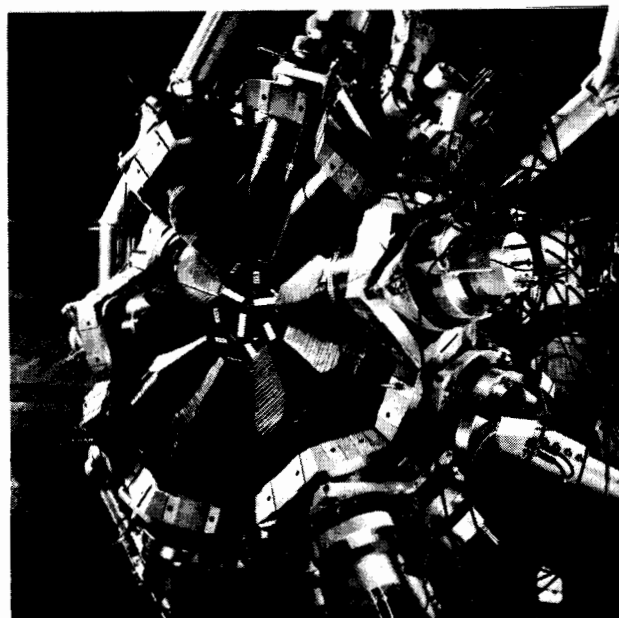


Fig.1 View of the Karlsruhe  $4\pi$  BaF<sub>2</sub> detector showing one hemisphere with the hexagonal and pentagonal detector modules. The sample for neutron capture studies will be located in the centre.

2. The Karlsruhe  $4\pi$  detector

The Karlsruhe  $4\pi$  BaF<sub>2</sub> detector (see Fig.1) is the first spherically symmetric setup made from barium fluoride crystals, which offers ~100% efficiency for gamma-ray energies up to 10 MeV. It is composed of 42 crystals, shaped as hexagonal and pentagonal truncated pyramids and forming a spherical shell with 20 cm inner diameter and 15 cm thickness. The final volume of each crystal is 1.5 l, corresponding to a weight of 7.5 kg. The crystals are cut from BaF<sub>2</sub> cylinders of about 2.5 l volume, which was the maximum size at the time when they were ordered. Each crystal is covered by a thin reflector and viewed by a phototube, thus representing a complete gamma-ray detector. The energy resolution of these individual modules is typically 10 - 11% at 0.662 and 4 - 5% at 6.13 MeV

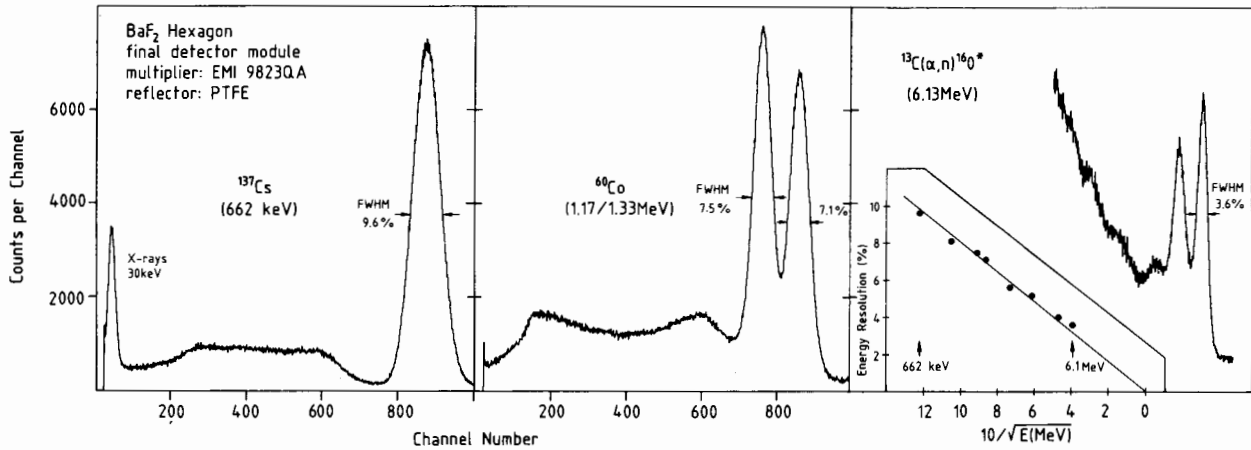


Fig.2 Gamma-ray spectra taken with an optimal detector module between 662 keV and 6.13 MeV.

gamma-ray energy, as illustrated in figure 2. At the same time, the  $\text{BaF}_2$  crystals provide for an excellent time resolution of 400 - 500 ps. Compared to the  $4\pi$  detectors made from  $\text{NaI}(\text{Tl})$  as the Oak Ridge spin spectrometer or the Heidelberg crystal ball detector, the present setup has a five times better time resolution at a similar resolution in gamma-ray energy.

The individual detector modules are fixed in a spherical honeycomb structure; this allows each module to be mounted and adjusted separately. The spherical detector is subdivided into two parts, which move on rails independent of each other over a maximum distance of  $\sim 1.5$  m. In this way, the detector can be opened for easy access of the samples or it can be shifted as a whole in order to change the flight path between neutron target and sample.

The  $4\pi$  detector is used as a gamma-ray calorimeter. In order to reduce backgrounds, a fast decision is made electronically within 20 ns whether the sum energy of a particular event deposited in the whole detector exceeds a threshold of typically 2 to 3 MeV. This is achieved by considering only the fast component of the scintillation light of all modules. The

corresponding sum energy signal is 10 ns wide and carries still an energy resolution of  $\sim 15\%$  at 3 MeV gamma-ray energy. When an event is accepted by the above condition, linear gates are opened for those modules that have fired in order to process the entire signals with high energy resolution. Simultaneously, a timing signal for the event is derived from a fast 42fold OR, which is triggered by constant fraction discriminators.

The complete detector is under computer control using CAMAC modules for constant fraction discriminators, delays, high voltage power supplies, linear gates, scalars, and multiplexers. This allows for automatic gain and delay adjustments, threshold settings etc. via computer software. During the experiments, long term stabilization is obtained making use of the internal calibration provided by the  $\alpha$ -lines from radium impurities in the crystals. These  $\alpha$ -signals can easily be separated from gamma-ray events by simple pulse shape analysis<sup>5</sup>.

Examples for the efficiency as well as gamma-ray and time resolution of the  $4\pi$  detector are given in figure 3. All measurements were made with a  $^{60}\text{Co}$  source and with 40 instead of 42 detector modules. Correspondingly, only a solid angle of 95%

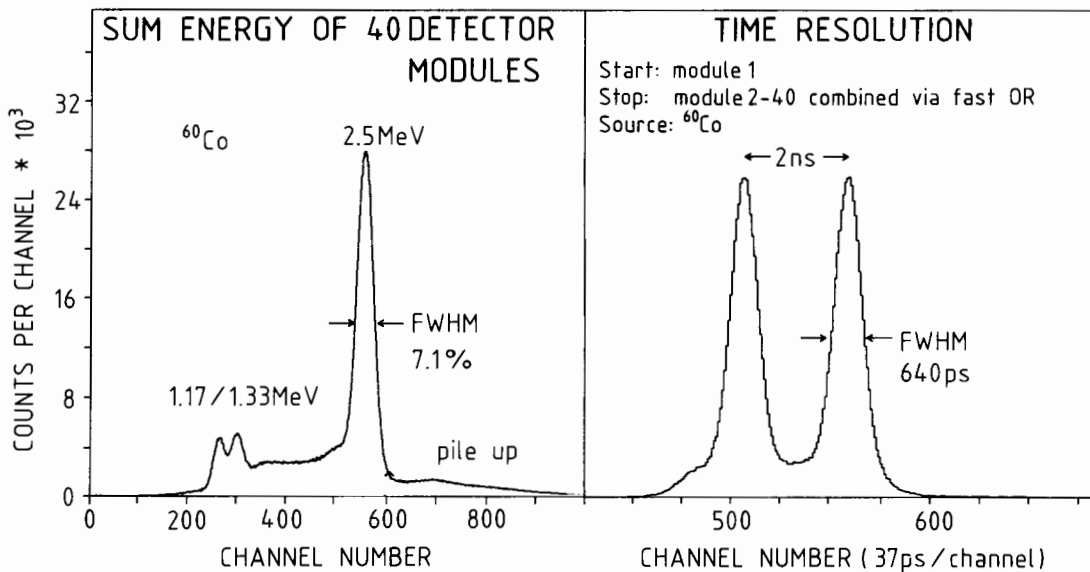


Fig.3 Gamma-ray energy and time resolution of the total detector (with 40 out of 42 modules,  $^{60}\text{Co}$  source).

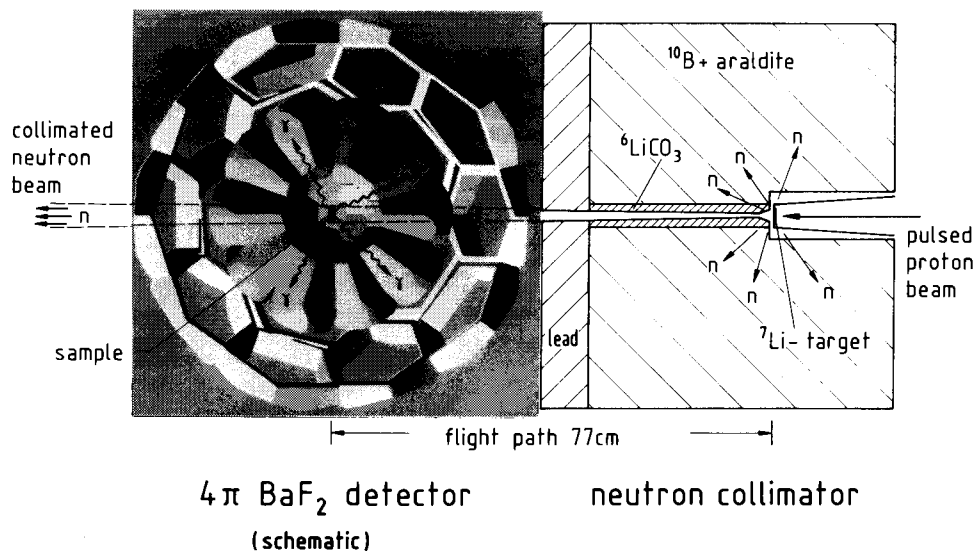


Fig.4 Schematic setup for the determination of neutron capture cross sections in the energy range from 3 to 200 keV.

of  $4\pi$  was covered by active crystals, leading to a 5% intensity of the individual lines compared to 90% in the sum peak. The observed energy resolution of 7.1% is slightly worse as expected from the average resolution of the individual modules. This difference is mainly due to the limited resolution of the gain stabilization as the high voltage supply for the photomultipliers can only be changed in steps of 1 V. A time resolution of 640 ps was measured for one reference module versus the rest of the detector, indicating a time resolution of 500 ps for the total detector. This value impressively illustrates the outstanding timing properties of BaF<sub>2</sub> crystals.

### 3. Test measurements: neutron capture in gold

The experimental setup for the measurement of neutron capture cross sections is sketched in figure 4. The pulsed proton beam of the Van de Graaff accelerator ( $E_p = 1.97$  MeV; rep. rate = 250 kHz;  $I_p = 2 \mu\text{A}$ ) falls on a metallic lithium target, producing a continuous neutron spectrum in the energy range from 3 to 200 keV via the  ${}^7\text{Li}(p,n){}^7\text{Be}$  reaction. A collimated neutron beam is produced by a carefully designed shield consisting mainly from boron,  ${}^6\text{Li}$ -carbonate, and araldite. The neutron beam crosses the detector through holes in opposite crystals and is 30 mm in diameter at its centre. (However, the present tests had to be made without those special modules). The neutron flight path was 77 cm.

During the measurements, two-dimensional spectra containing the sum energy of the gamma-ray cascade versus the time of flight were stored on-line. In addition, the same data were also recorded in list mode on magnetic tape for a more detailed off-line analysis. A 42 bit word per event was added to the list mode data, by which the particular modules that have contributed to that event were identified. With this information it was later possible to study the multiplicity distribution.

The upper part of figure 5 shows such a two-dimensional spectrum taken with a 1 mm thick gold sample. The peak at a sum energy of 6.5 MeV

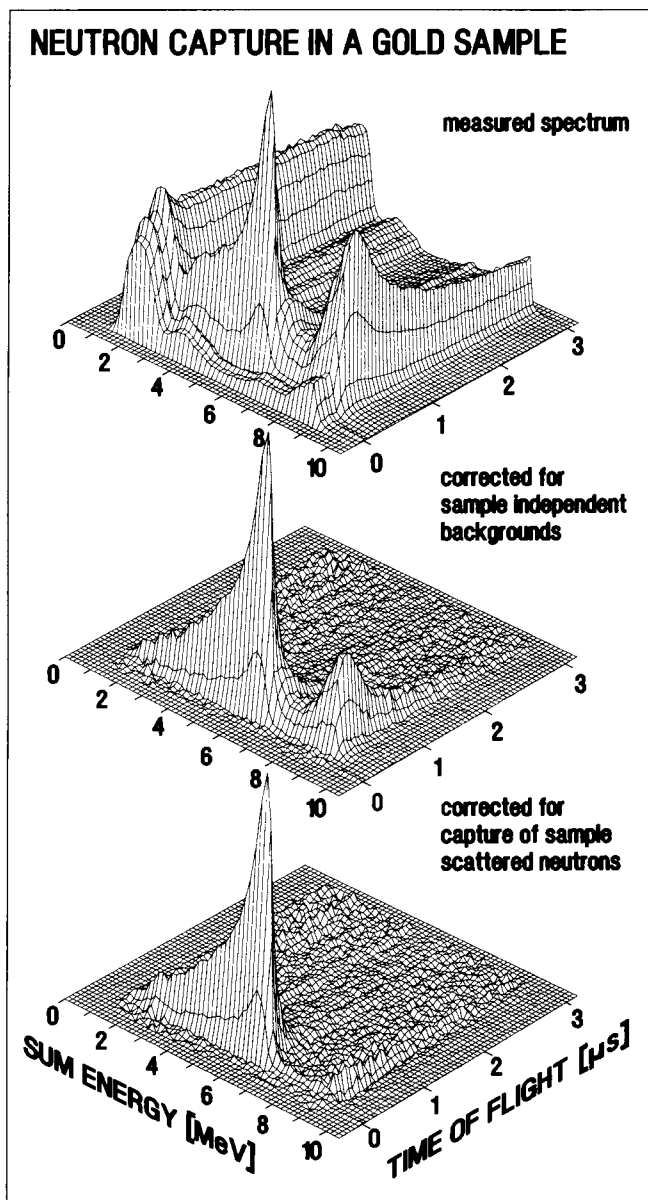


Fig.5 Two-dimensional spectra of sum energy versus time of flight measured with a 1 mm thick gold sample.

corresponds to capture in gold and is clearly visible above the background. The time-independent background at low sum energies is mainly due to the radium impurities in the BaF2 crystals, while the high energy component originates from scattered neutrons, which are captured in barium. About 60% of that latter component is due to  $^{135}\text{Ba}$ , for which the neutron binding energy is 9.1 MeV.

The spectrum in the mid part of figure 5 was obtained by subtracting the sample-independent backgrounds, which were measured after the sample was removed from the neutron beam. The only remaining events are therefore those from neutron capture in gold and a residual background from sample scattered neutrons, which are captured predominantly in the barium isotopes of the scintillator. The following features that are essential for our new setup can be illustrated by means of this part of the figure:

(i) Most of the background due to sample scattered neutrons is located at a sum energy of  $\sim 9$  MeV, well separated from primary capture events. The majority of isotopes that are important for nuclear astrophysics having binding energies of 6 to 7 MeV, this separation facilitates many future experiments.

(ii) The background due to sample scattered neutrons is spread over a time interval of  $\sim 3 \mu\text{s}$ . Therefore, only a smaller part falls in the time window of about 400 ns occupied by primary capture events. The larger spread for scattered neutrons is caused by the fact that these neutrons are captured only after having been scattered for about 20 times on average<sup>2</sup>. Note, that this feature is lost in experiments, where the neutron flight times are of the order of 5  $\mu\text{s}$ , e.g. at electron linear accelerators.

(iii) The integral number of background events is compatible with the number of primary capture events. As the cross section for neutron scattering in gold is about ten times larger than that for capture, this shows that  $\sim 90\%$  of the scattered neutrons escape from the BaF2 crystals in good agreement with previous Monte Carlo calculations<sup>2</sup>.

If NaI(Tl) were used instead of BaF2, this would have the consequence that practically all neutrons were captured without any significant time delay because of the large capture cross section of iodine. As the neutron binding energies of gold and iodine are almost equal, the primary events would have been completely buried under a background, which on average is 100 times larger compared to the situation with the BaF2 detector. Any shielding of scattered neutrons, e.g. a spherical layer of  $^{10}\text{B}$  around the sample, significantly degrades the resolution in gamma-ray energy as in case of the ROMASCHKA detector.

In the lower part of figure 5 the remaining background due to sample scattered neutrons has been eliminated by subtraction of a spectrum measured with a graphite sample. As a result, one obtains a clear signature for the capture events in gold. The projected pulse height spectrum shows that about 50% of all events appear in the full energy peak at the binding energy, while more than 90% are above 3 MeV. The corresponding tail will be further reduced, when all 42 detector modules are available. As only 95% of  $4\pi$  are covered by BaF2 at present, there is a rather high probability that one of the gamma-rays of a cascade escapes detection, because the average multiplicity for gold is  $\sim 4$ .

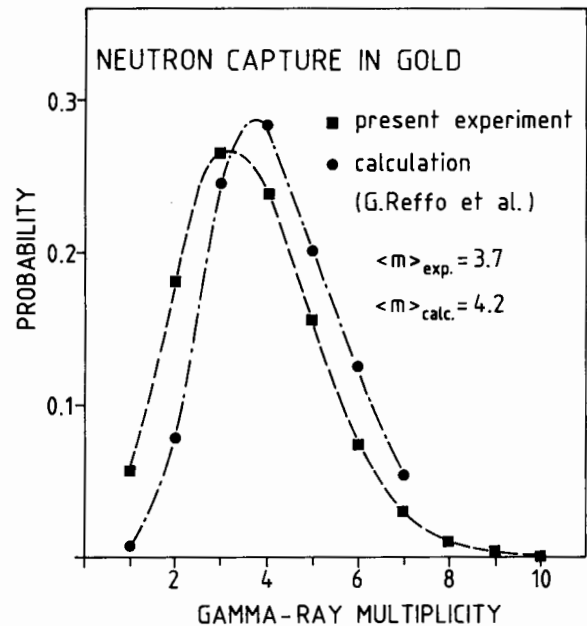


Fig.6 Experimental distribution of cascade multiplicities following neutron capture in gold compared to a previous calculation<sup>6</sup>.

Figure 6 shows the preliminary results for the multiplicity. The experimental points represent the number of modules that have fired in a particular event, and are not yet corrected for detector-detector scattering, the limited solid angle of  $95\%$  of  $4\pi$ , and the threshold energy of  $\sim 60$  keV for the individual modules. In view of all these effects, there is remarkably good agreement with a calculation by Reffo et al.<sup>6</sup>. Most of the observed difference may be due to the fact that the gamma-ray transitions between the first two excited states in  $^{198}\text{Au}$  are included in the calculation, but fall below the experimental threshold because of their small energies of 35 and 55 keV.

#### 4. Future

First quantitative measurements with the new detector are scheduled for the mid of 1988 and will be on the monotopic elements Nb, Rh, and Ta. These experiments are intended to further optimize the setup and to resolve persisting discrepancies among previous results. At the next stage we plan to investigate the cross sections of the tellurium and samarium isotopes, which are of key importance for stellar nucleosynthesis by the s-process.

#### References

1. K. Wisshak, F. Käppeler, H. Müller: Nucl. Instr. Meth. A251, 101 (1986)
2. K. Wisshak, F. Käppeler: Proc. Int. Conference on Nuclear Data for Basic and Applied Science (Santa Fe 1985), Radiation Effects 95, 1319 (1986)
3. F. Käppeler: contribution IJ02, this conference
4. G.V. Muradyan, Yu.V. Adamchuk, Yu.G. Shchepkin, M.A. Voskanyan: Nucl. Sci. Eng. 90, 60 (1985)
5. K. Wisshak, F. Käppeler: Nucl. Instr. Meth. 227 91 (1984)
6. G. Reffo, F. Fabbri, K. Wisshak, F. Käppeler: Nucl. Sci. Eng. 80, 630 (1982)